



Template-Free Synthesis of One-Dimensional g-C₃N₄ Chain Nanostructures for Efficient Photocatalytic Hydrogen Evolution

Mingyi Zhang¹, Ye Sun¹, Xin Chang¹ and Peng Zhang^{2*}

¹Key Laboratory for Photonic and Electronic Bandgap Materials, Ministry of Education, School of Physics and Electronic Engineering, Harbin Normal University, Harbin, China, ²School of Materials Science and Engineering, Zhengzhou University, Zhengzhou, China

OPEN ACCESS

Edited by:

Kangle Lv,
South-Central University for
Nationalities, China

Reviewed by:

Kezhen Qi,
Shenyang Normal University, China
Li Yuhan,
Chongqing Technology and Business
University, China
Li Xiaofang,
Wuhan University, China

*Correspondence:

Peng Zhang
zhangp@zzu.edu.cn

Specialty section:

This article was submitted to
Catalysis and Photocatalysis,
a section of the journal
Frontiers in Chemistry

Received: 13 January 2021

Accepted: 04 February 2021

Published: 15 March 2021

Citation:

Zhang M, Sun Y, Chang X and Zhang P
(2021) Template-Free Synthesis of
One-Dimensional g-C₃N₄ Chain
Nanostructures for Efficient
Photocatalytic Hydrogen Evolution.
Front. Chem. 9:652762.
doi: 10.3389/fchem.2021.652762

The development of graphite-carbon nitride (g-C₃N₄) photocatalyst is of great significance for various visible utilization applications. Control the nanostructures of g-C₃N₄ can tailor its photocatalytic performance. In this paper, one-dimensional chain-like g-C₃N₄ was successfully synthesized by heat-induced polymerization of melamine which was saturated in ethylene glycol. The photocatalytic hydrogen production rate (HER) of the prepared g-C₃N₄ chain enhanced about 3 times than that of bulk g-C₃N₄, increasing from 9.6 μmolh⁻¹ to 28.7 μmolh⁻¹. The improved photocatalytic activity of the g-C₃N₄ chain was attributed to the advantages of porosity and nanostructure. The extraordinary nanopores result in an enlarged specific surface area for adsorption and the production of abundantly available channels for charge transfer. The one-dimensional chain-like structure can facilitate the exposure of internal/external active sites as many as possible, and induce the directional migration of charge carriers.

Keywords: g-C₃N₄, one-dimensional (1D), photocatalytic, template-free, hydrogen evolution

INTRODUCTION

With the rapid pace of industrialization and urbanization growing in the past few decades, global crises related to environmental degradation and energy shortage have become the most critical topics to the world and threaten the survival environment of humankind (Yu et al., 2017; Yu et al., 2019). Photocatalytic water splitting for hydrogen evolution has been considered as a sustainable strategy to convert and store plentiful solar energy for future energy requirements (Wang et al., 2009; Wang et al., 2012; Ong et al., 2016). In the last several decades, graphitic carbon nitride (g-C₃N₄) the organic semiconductor showed a specific graphite-like sp²-bonded C–N structure that exhibits significant potential in the field of CO₂ conversion, water splitting, and environmental remediation on account of its inexpensive preparation, brilliant visible light response, thermal stability, and well-developed electronic band structure (Ding et al., 2018; He et al., 2019; Rong et al., 2020; Shu et al., 2020; Zhang D. et al., 2020). However, g-C₃N₄ accompanied by the defaults such as poor quantum efficiency, low specific surface area, and rapid charge recombination have adversely affected the photocatalytic application of g-C₃N₄.

A large number of strategies acting to resolve these problems and reinforce the photocatalytic performances of g-C₃N₄, involving non-metal element doping [S (Cao et al., 2018), O (Jiang et al., 2019), V (Ding et al., 2013), B (Yan et al., 2010), etc.], noble metals decoration [Pd (Wang et al., 2011) Pt (Maeda et al., 2009) and Au (Li et al., 2012)], heterojunction designing (Liang et al., 2019; Shi et al.,

2020a; Shi et al., 2020b) and coupling with graphene (Li et al., 2013; Han et al., 2017). Expect for the capacity of g-C₃N₄ to collaborate with other materials, layers structure configuration is deemed as a prospective method to compound g-C₃N₄ as they can accelerate the diffusion of reactant, strengthen the light harvesting, expand the exposed surface areas, and promote the charge delivery.

Generally speaking, microstructural g-C₃N₄ photocatalysts with controllable morphology and structure can be divided into six categories: mesoporous (Zhao et al., 2018; Chen et al., 2019), nanosheets (Yang et al., 2017; Gao et al., 2018), nanorods (Cui et al., 2012; Bai et al., 2013), nanotubes (Gao et al., 2012), and nanospheres (Zheng et al., 2015). Among them, one-dimensional (1D) nanostructured photocatalyst, especially fabricating 1D photocatalyst with large surface area, is especially interested as the charges can vectorially transfer along with the 1D structure (Tahir et al., 2014).

After discovering the carbon nanotubes, 1D nanostructures (lines, rods, tubes, strips, fibers, etc) have attracted extensive attention from researchers. 1D nanostructures have greatly satisfied the increasing demand for microelectronics and optoelectronic devices such as optical waveguides, field-effect transistors, and photodetectors in recent years. 1D nanostructures showed brilliant phonon, gas sensitivity, field emission, photoconductivity, and electron transport performance due to their higher surface volume ratio and more active position. Furthermore, the growth of 1D nanostructures has an immense effect on improving the mechanical energy, thermal and electrical capabilities of materials. Because nanoparticles in 1D nanostructures are interconnected in three dimensions, an extremely fast interparticle, vectorially transport of photogenerated charge carriers (electrons and holes) is likely to emerge through the grain boundaries. This represents that the redox reaction sites are far away related to the photoexcitation sites, which seems to be responsible for the high activities of photocurrent generation and hydrogen production.

In the present work, 1D g-C₃N₄ chain nanostructures were obtained by regulating the saturation of melamine and ethylene glycol solution for photocatalytic hydrogen evolution. The enhanced photocatalytic properties are known to be caused by an extension of the life of the photoinduced charge carrier. In addition, increasing specific surface area is also a vital factor in promising photocatalytic performance. Owing to the composite method is convenient, environmentally friendly, and low-cost, it is suitable for an expanded range of practical applications.

EXPERIMENTAL

Synthesis of the g-C₃N₄ Chain Nanostructures

The one-dimensional g-C₃N₄ chain nanostructures were prepared by a controllable approach. Firstly, excessive amounts of melamine powders (3.0 g) were dissolved in 60 ml of ethylene glycol to form a saturated solution at room temperature. Subsequently, add 1 ml of concentrated nitric

acid solution to 59 ml of water, drop by drop add the solution to 20 ml of supernatant and stir continuously until a white flocculent precipitate is obtained. The white flocculent precipitate was bleached with ethanol five times to remove nitric acid and ethylene glycol. Lastly, the collected sample was transferred into the muffle furnace for heating 2 h at 550°C with a heating rate of 20°C·min⁻¹. Meanwhile, as the contrast sample, the bulk g-C₃N₄ was obtained by the heating process at 550°C for 2 h with a heating rate of 20°C·min⁻¹ of the melamine powders.

Characterization

The crystal structure was characterized by X-ray diffraction (XRD, D/max2600, Rigaku, Japan) using the Cu K α radiation ($k = 1.5418 \text{ \AA}$). The morphologies of one-dimensional g-C₃N₄ chain nanostructures were characterized by scan electron microscopy (SEM, SU70, Hitachi, Japan). And specific surface areas of the one-dimensional g-C₃N₄ chain nanostructures were measured by a Micromeritics ASAP 2010 instrument and analyzed by the Brunauer–Emmett–Teller (BET) method. Photoluminescence (PL) spectra of photocatalysts were performed on a Jobin Yvon HR800 micro-Raman spectrometer including a 325 nm line from a He–Cd laser. UV-Vis diffuse reflectance spectra (DRS) of the samples are obtained by using a UV-Vis-IR spectrometer (Perkin-Elmer, Lambda 850). Photocurrent measurements were characterized by CHI 660 E electrochemical workstation (Chenhua, Shanghai) by applying a three-electrode cell accompanied by a visible light source. A platinum filament, Ag/AgCl electrode, and 0.2 M of Na₂SO₄ were acted as the counter electrode, reference electrode, and an electrolyte solution, separately. The as-fabricated sample mixed a certain amount of Nafion solution was painted on FTO glass as a working electrode (the effective area was 1 cm \times 1 cm).

Photocatalytic Test

Photocatalytic H₂ evolution was injected into a 250 ml of quartz reactor with a visible-light source irradiation. As a typical synthesis experiment, 0.1 g of photocatalyst with a certain Pt cocatalyst (1 wt%) was dispersed in a mixed solution of aqueous solution (90 ml) and methanol (10 ml). The amount of H₂ evolution was measured in a gas chromatograph (GC-2014C Shimadzu Corp., N₂ as carrier gas). The time interval of sampling was performed at 40 min during the water splitting process.

RESULTS AND DISCUSSION

The morphology of the as-fabricated products was scrutinized by scanning electron microscope (SEM). **Figure 1A** depicts the SEM image of the as-prepared bulk g-C₃N₄, in which the sample possesses a hierarchical component with a particle size of greater than 20 μm . However, in **Figure 1B**, we found that the morphology of g-C₃N₄ changed greatly compared with the bulk structure, and a new one-dimensional chain structure appeared. It can be illustrated from **Figure 1B** that the lengths of these irregular-oriented chains g-C₃N₄ one-dimensional structure could reach dozens of micrometers, and the diameters of those fibers range from 1 to 2 μm . Each one-dimensional structure was

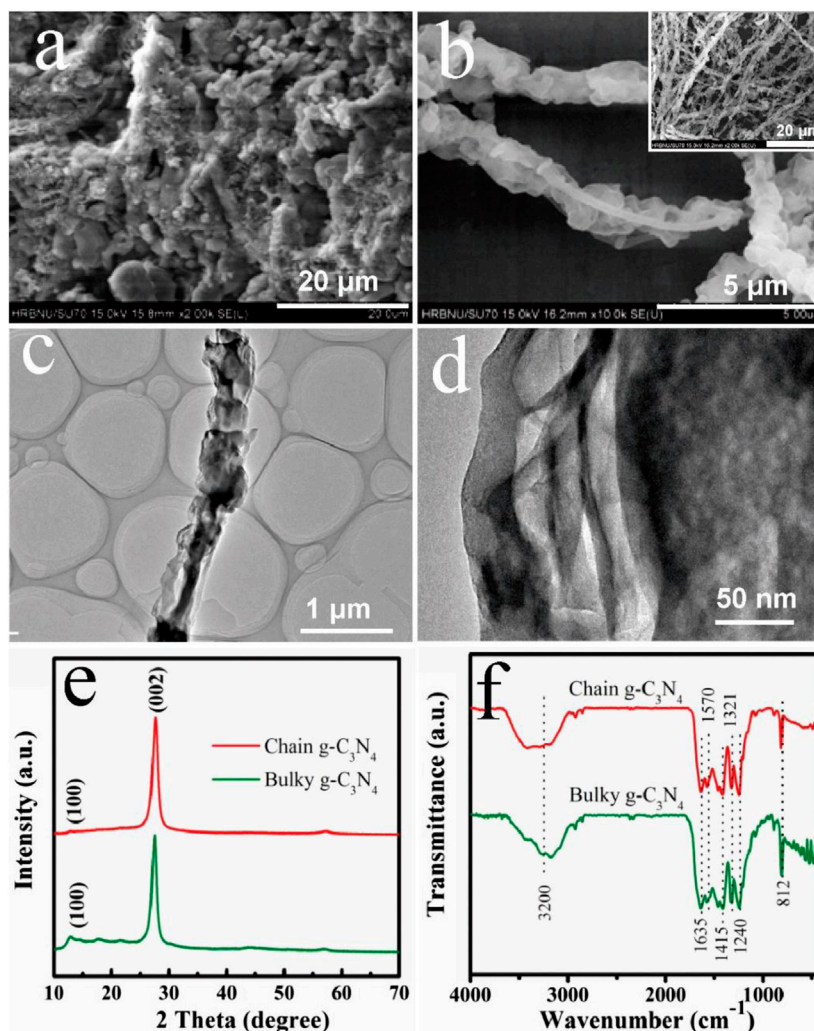


FIGURE 1 | SEM images of (A) bulky g-C₃N₄ and (B) chain g-C₃N₄ at low and high magnification, and (C, D) TEM image of chain g-C₃N₄ at low and high magnification; (E) XRD and (F) FT-IR patterns of bulky g-C₃N₄ and pearl-chain g-C₃N₄.

separated from each other, and further secondary structures could be found. Through the observation of the morphology characteristics of the two structures, we can infer that the chain g-C₃N₄ material will possess a vast specific surface area, which is more conducive to enhance the photocatalytic performance. The transmission electron micrographs of chain g-C₃N₄ are shown in **Figures 1C,D**. We can see the chain g-C₃N₄ presents a similar sponge hole that exists on the surface of the chain g-C₃N₄, the morphology can effectively improve the capacity in the course of the photocatalytic reaction area. Meanwhile, the product can shorten the time and distance of the charge transfer, and promote the charge separation order to improve the photocatalytic activity of the material. As we all known, in the pyrolysis period of supramolecular precursor, the by-products were formed with varieties of gases gradually released, giving rise to the nitrogen defects obtained in the framework of g-C₃N₄.

X-ray diffraction (XRD) patterns for chain g-C₃N₄ and bulky g-C₃N₄ are expressed in **Figure 1E**. Obviously, both patterns

contain two diffraction peaks, which are located at 13.2° and 27.6°, respectively. The former peak at 13.2° could be indexed as (100) lattice plane, which is associated with interlayer stacking. The corresponding interlayer spacing value has been calculated to be 0.676 nm. And the later peak at 27.6° is a feature interlayer stacking peak of aromatic systems, which could be indexed as (002) lattice plane. The calculated interplanar distance of aromatic units is 0.326 nm (Li et al., 2020a; Zhang et al., 2020b).

Figure 1F shows the Fourier transform infrared (FT-IR) spectra of the as-prepared samples. The FT-IR spectra of the synthesized chain g-C₃N₄ were compared to the bulky g-C₃N₄ exhibit with similar characteristics. The FT-IR the bands located at 1,240, 1,321, 1,415 cm⁻¹, and 1,570 cm⁻¹ are mainly from the typical stretching modes of C-N heterocycles. And the band at 810 cm⁻¹ is attributed to out-of-plane bending modes of C-N heterocycles. The C-N stretching mode has IR band at 1,635 cm⁻¹. And the broadband near 3,200 cm⁻¹ corresponds

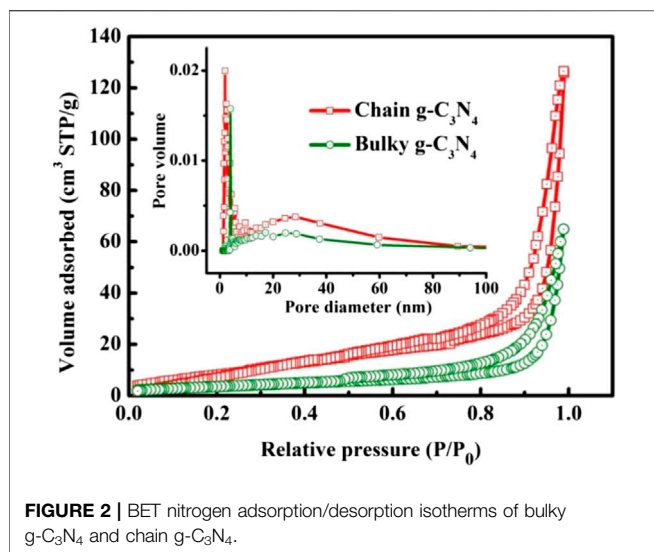


FIGURE 2 | BET nitrogen adsorption/desorption isotherms of bulky g-C₃N₄ and chain g-C₃N₄.

to the stretching modes of terminal NH₂ or NH groups at the defect sites of the aromatic ring (Li et al., 2020b; Li et al., 2020c).

The exposed surface area and pores distribution of chain g-C₃N₄ and bulky g-C₃N₄ were further researched. The adsorption-desorption isotherm curve of chain g-C₃N₄ and bulky g-C₃N₄ demonstrate the type IV curve, as shown in **Figure 2**, indicating the presence of uniform mesoporous with high specific surface area and large total pore volume. The specific surface area of chain g-C₃N₄ was counted to be 47.85 m²g⁻¹ through the Brunauer-Emmett-Teller (BET), which is approximately three times larger than pure bulky g-C₃N₄ (16.15 m²g⁻¹). The inset in **Figure 2** exhibits the pore-size distribution of the chain g-C₃N₄ and bulky g-C₃N₄. The pore distribution for chain g-C₃N₄ is mainly located at 2.46 nm, and the pore volume is 0.233 cm³g⁻¹. But for the bulky g-C₃N₄, the pore volume is just 0.097 cm³g⁻¹. The mesoporous structure and large surface area of the chain g-C₃N₄ are conducive to the absorption of more active substances and reactants on the surface, enhancing the photocatalytic reaction. Therefore, we can assume that the chain g-C₃N₄ material can have superior photocatalytic activity.

The UV-vis diffuse reflectance spectroscopy illustrated by **Figure 3**. from the (ahv)^{1/2} vs. photon energy (hv) plot (Hou et al., 2020; Li et al., 2020d; Wang et al., 2020a; Zhang et al., 2020a; Zhang Y. et al., 2020), the optical bandgap of chain g-C₃N₄ and bulk g-C₃N₄ was calculated to be approximate 2.88 and 2.93 eV, respectively. When the particle size descends to a certain value, the electron energy level near the Fermi energy level of the metal changes from quasi-continuous to discrete energy level (Miao et al., 2019; Huang et al., 2020b; Wu et al., 2020; Zhang S. et al., 2020), and the highest occupied molecular orbital (HOMO) and lowest unoccupied molecular orbital (LUMO) of the nano-semiconductor particles have discontinuous energy gap, which leads to the blue shift of the chain g-C₃N₄.

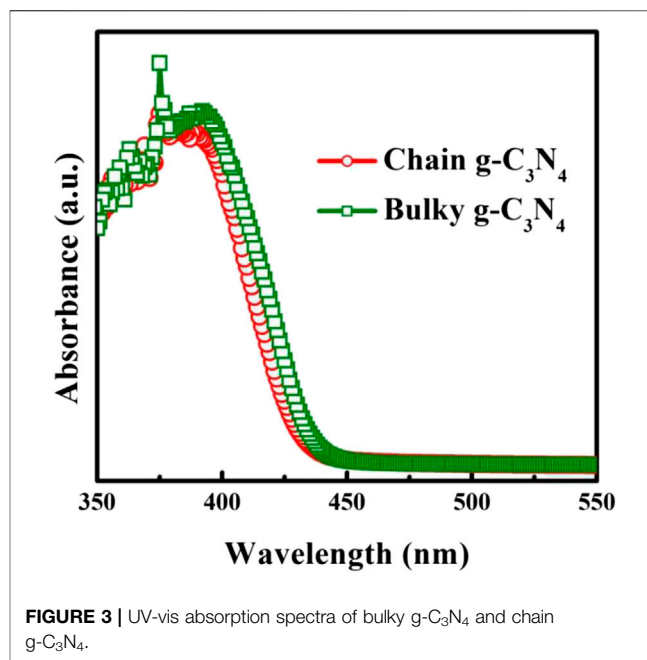


FIGURE 3 | UV-vis absorption spectra of bulky g-C₃N₄ and chain g-C₃N₄.

According to mentioned above, the prepared chain g-C₃N₄ has a one-dimensional superstructure with a wide surface area, making it a more suitable candidate material for photocatalytic H₂ production. To evaluate the photocatalytic performance of chain g-C₃N₄ photocatalyst with the visible light irradiation, the H₂ production performance was tested and compared with that of bulky g-C₃N₄ photocatalytic performance was compared.

As the result shown in **Figure 4A**, the H₂ evolution rate of the bare bulky g-C₃N₄ sample was measured to be 9.6 μmolh⁻¹, separately. However, the photocatalytic properties of chain g-C₃N₄ were markedly improved, and the H₂ generation rate increased as high as 28.7 μmolh⁻¹. The chain g-C₃N₄ sample shows rather superior photocatalytic activity for H₂ evolution, which could be ascribed to its vaster surface area (**Figure 2**). **Figure 4B** shows the stability of the photocatalytic H₂ production system using chain g-C₃N₄ as the photocatalyst under visible light irradiation. Therefore, we studied the chemical stability of chain g-C₃N₄, as described in **Figure 4B**. After four consecutive cycle experiments, we found that the evolution rate of the chain g-C₃N₄ did not decline significantly, indicating that the material has good chemical stability.

The key factor of photocatalytic reaction is the effective generation and rapid separation of photoexcited carriers (Huang et al., 2020a; Li X. et al., 2020; Wang L. et al., 2020; Wang et al., 2020b; Zhang et al., 2020c). The optical performances of the samples were measured by photoluminescence (PL). The intensity of PL spectra can state the extent of the recombination of photo-generated charges. In **Figure 5A**, it illustrates bulky g-C₃N₄ emerge severe charge recombination, while the PL spectrum of chain g-C₃N₄ is intense quenched (**Figure 5A**). The reorganizing of the photo-generated e-h pairs of chain g-C₃N₄ can be restrained. The restraining of the e-h pair

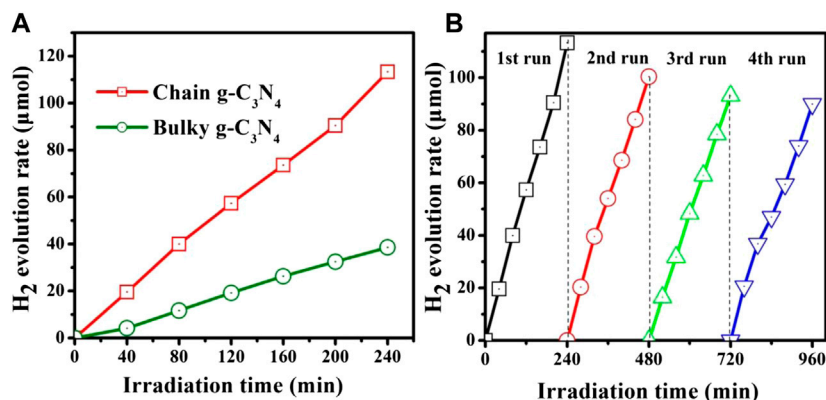


FIGURE 4 | (A) The amount of hydrogen evolution over the bulky g-C₃N₄ and chain g-C₃N₄, and **(B)** cycling test of photocatalytic hydrogen evolution under visible light.

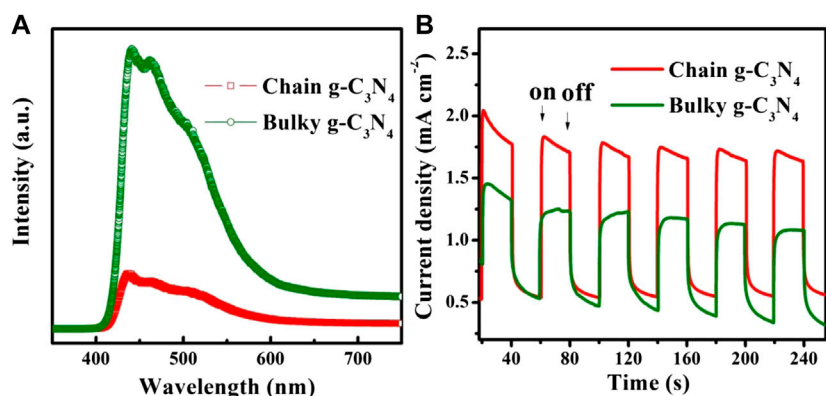


FIGURE 5 | (A) PL spectra and **(B)** photocurrents spectra of bulky g-C₃N₄ and chain g-C₃N₄.

recombination is powerfully verified by the increased photocurrents for chain g-C₃N₄, as shown in **Figure 5B**. Apparently, the chain g-C₃N₄ was provided with a better separation efficiency of e-h pairs.

To further confirm the ability of several samples to separate and transfer charges and to respond to light (Cheng et al., 2019; Li et al., 2021), we performed photocurrent tests on them, as shown in **Figure 5B** six cycles were tested under $\lambda > 420$ nm xenon lamp. As can be seen from the diagram, two working electrode transient photocurrent response of bulky g-C₃N₄ and chain g-C₃N₄ were obtained through these six cycles. It can be seen that the transient photocurrent spectrum of the chain g-C₃N₄ electrode was much better than the bulky g-C₃N₄. Test results indicate that chain g-C₃N₄ greatly improves the separation of interface carriers. The photocurrent research consequences coincide with the impedance and photoluminescence research consequences, demonstrating that the chain g-C₃N₄ material will have better photocatalytic performance.

CONCLUSION

In summary, we proposed an annealing method to achieve bulky g-C₃N₄ and chain g-C₃N₄ utilizing melamine as reactant materials. The chain g-C₃N₄ nanostructures illustrated improvement on the photocatalytic H₂ production under visible light irradiation owing to unique inimitable one-dimensional structure, high specific surface area, excellent light-harvesting properties, and low recombination rate of electron-hole pairs. This simple preparation and facile composition of one-dimensional g-C₃N₄ nanostructures demonstrate a promising candidate for exploring more actual applications of carbon nitride.

DATA AVAILABILITY STATEMENT

The original contributions presented in the study are included in the article/Supplementary Material, further inquiries can be directed to the corresponding author.

AUTHOR CONTRIBUTIONS

All authors listed have made a substantial, direct, and intellectual contribution to the work and approved it for publication.

REFERENCES

- Bai, X., Wang, L., Zong, R., and Zhu, Y. (2013). Photocatalytic activity enhanced via g-C₃N₄ nanoplates to nanorods. *J. Phys. Chem. C* 117, 9952–9961. doi:10.1021/jp402062d
- Cao, S., Fan, B., Feng, Y., Chen, H., Jiang, F., and Wang, X. (2018). Sulfur-doped g-C₃N₄ nanosheets with carbon vacancies: general synthesis and improved activity for simulated solar-light photocatalytic nitrogen fixation. *Chem. Eng. Technol.* 353, 147–156. doi:10.1016/j.cej.2018.07.116
- Chen, X., Shi, R., Chen, Q., Zhang, Z., Jiang, W., Zhu, Y., et al. (2019). Three-dimensional porous g-C₃N₄ for highly efficient photocatalytic overall water splitting. *Nano Energy* 59, 644–650. doi:10.1016/j.nanoen.2019.03.010
- Cheng, J., Hu, Z., Li, Q., Li, X., Fang, S., Wu, X., et al. (2019). Fabrication of high photoreactive carbon nitride nanosheets by polymerization of amidinourea for hydrogen production. *Appl. Catal. B-Environ.* 245, 197–206. doi:10.1016/j.apcatb.2018.12.044
- Cui, Y., Ding, Z., Fu, X., and Wang, X. (2012). Construction of conjugated carbon nitride nanoarchitectures in solution at low temperatures for photoredox catalysis. *Angew. Chem. Int. Ed. Engl.* 51, 11814–11818. doi:10.1002/anie.201206534
- Ding, G., Wang, W., Jiang, T., Han, B., Fan, H., and Yang, G. (2013). Highly selective synthesis of phenol from benzene over a vanadium-doped graphitic carbon nitride catalyst. *ChemCatChem* 5, 192–200. doi:10.1002/cctc.201200502
- Ding, J., Xu, W., Wan, H., Yuan, D., Chen, C., Wang, L., et al. (2018). Nitrogen vacancy engineered graphitic C₃N₄-based polymers for photocatalytic oxidation of aromatic alcohols to aldehydes. *Appl. Catal. B-Environ.* 221, 626–634. doi:10.1016/j.apcatb.2017.09.048
- Gao, M., Feng, J., Zhang, Z., Gu, M., Wang, J., Zeng, W., et al. (2018). Wrinkled ultrathin graphitic g-C₃N₄ nanosheets for photocatalytic degradation of organic wastewater. *ACS Appl. Nano Mater.* 1, 6733–6741. doi:10.1021/acsnm.8b01528
- Gao, J., Zhou, Y., Li, Z., Yan, S., Wang, N., and Zou, Z. (2012). High-yield synthesis of millimetre-long, semiconducting carbon nitride nanotubes with intense photoluminescence emission and reproducible photoconductivity. *Nanoscale* 4, 3687–3692. doi:10.1039/c2nr30777d
- Han, Q., Cheng, Z., Gao, J., Zhao, Y., Zhang, Z., Dai, L., et al. (2017). Mesh-on-mesh graphitic-C₃N₄@graphene for highly efficient hydrogen evolution. *Adv. Funct. Mater.* 27, 1606352. doi:10.1002/adfm.201606352
- He, S., Xiao, K., Chen, X.-Z., Li, T., Ouyang, T., Wang, Z., et al. (2019). Enhanced photoelectrocatalytic activity of direct Z-scheme porous amorphous carbon nitride/manganese dioxide nanorod arrays. *J. Colloid Interface Sci.* 557, 644–654. doi:10.1016/j.jcis.2019.09.035
- Hou, R., Zhang, S., Zhang, P., Zhang, Y., Zhang, X., Li, N., et al. (2020). Ti₃C₂ MXene as an “energy band bridge” to regulate the heterointerface mass transfer and electron reversible exchange process for Li-S batteries. *J. Mater. Chem. A* 8, 25255. doi:10.1039/d0ta06695h
- Huang, J., Du, J., Du, H., Xu, G., and Yuan, Y. (2020a). Control of nitrogen vacancy in g-C₃N₄ by heat treatment in an ammonia atmosphere for enhanced photocatalytic hydrogen generation. *Acta. Phys. Chim. Sin.* 36, 1905056. doi:10.3866/pku.whxb201905056
- Huang, J., Liu, T., Wang, R., Zhang, M., Wang, L., She, H., et al. (2020b). Facile loading of cobalt oxide on bismuth vanadate: proved construction of p-n junction for efficient photoelectrochemical water oxidation. *J. Colloid Interface Sci.* 570, 89–98. doi:10.1016/j.jcis.2020.02.109
- Jiang, Y., Sun, Z., Tang, C., Zhou, Y., Zeng, L., and Huang, L. (2019). Enhancement of photocatalytic hydrogen evolution activity of porous oxygen doped g-C₃N₄ with nitrogen defects induced by changing electron transition. *Appl. Catal. B-Environ.* 240, 30–38. doi:10.1016/j.apcatb.2018.08.059

FUNDING

This work was supported by the National Natural Science Foundation of China (51872068), Heilongjiang Natural Science Foundation (E2018051).

- Li, X.-H., Wang, X., and Antonietti, M. (2012). Mesoporous g-C₃N₄ nanorods as multifunctional supports of ultrafine metal nanoparticles: hydrogen generation from water and reduction of nitrophenol with tandem catalysis in one step. *Chem. Sci.* 3, 2170–2174. doi:10.1039/c2sc20289a
- Li, Y., Zhang, H., Liu, P., Wang, D., Li, Y., and Zhao, H. (2013). Cross-linked g-C₃N₄/rGO nanocomposites with tunable band structure and enhanced visible light photocatalytic activity. *Small* 9, 3336–44. doi:10.1002/sml.201203135
- Li, X., Wang, B., Wang, B., Yin, W., Di, J., Xia, J., et al. (2020). Cu²⁺ modified g-C₃N₄ photocatalysts for visible light photocatalytic properties. *Acta Phys. Chim. Sin.* 36, 1902001. doi:10.3866/pku.whxb201902001
- Li, Y., Gu, M., Shi, T., Cui, W., Zhang, X., Dong, F., et al. (2020a). Carbon vacancy in C₃N₄ nanotube: electronic structure, photocatalysis mechanism and highly enhanced activity. *Appl. Catal. B-Environ.* 262, 118281. doi:10.1016/j.apcatb.2019.118281
- Li, Y., Gu, M., Zhang, M., Zhang, X., Lv, K., Liu, Y., et al. (2020b). C₃N₄ with engineered three coordinated (N_{3C}) nitrogen vacancy boosts the production of ¹O₂ for efficient and stable NO photo-oxidation. *Chem. Eng. J.* 389, 124421. doi:10.1016/j.cej.2020.124421
- Li, Y., Gu, M., Zhang, X., Fan, J., Lv, K., Carabineiro, S. A. C., et al. (2020c). 2D g-C₃N₄ for advancement of photo-generated carrier dynamics: status and challenges. *Mater. Today* 41, 270–303. doi:10.1016/j.mattod.2020.09.004
- Li, Y., Zhang, P., Wan, D., Xue, C., Zhao, J., and Shao, G. (2020d). Direct evidence of 2D/1D heterojunction enhancement on photocatalytic activity through assembling MoS₂ nanosheets onto super-long TiO₂ nanofibers. *Appl. Surf. Sci.* 504, 144361. doi:10.1016/j.apsusc.2019.144361
- Li, K. N., Zhang, M. X., Ou, X. Y., Li, R. N., Li, Q., Fan, J. J., et al. (2021). Strategies for the fabrication of 2D carbon nitride nanosheets. *Acta. Phys. Chim. Sin.* 37, 2008010. doi:10.3866/PKU.WHXB202008010
- Liang, S., Zhang, D., Pu, X., Yao, X., Han, R., Yin, J., and Ren, X. (2019). A novel Ag₂O/g-C₃N₄ p-n heterojunction photocatalysts with enhanced visible and near-infrared light activity. *Sep. Purif. Technol.* 210, 786–797. doi:10.1016/j.seppur.2018.09.008
- Maeda, K., Wang, X., Nishihara, Y., Lu, D., Antonietti, M., and Domen, K. (2009). Photocatalytic activities of graphitic carbon nitride powder for water reduction and oxidation under visible light. *J. Phys. Chem. C* 113, 4940–4947. doi:10.1021/jp809119m
- Miao, F., Lu, N., Zhang, P., Zhang, Z., and Shao, G. (2019). Multidimension-controllable synthesis of ant nest-structural electrode materials with unique 3D hierarchical porous features toward electrochemical applications. *Adv. Funct. Mater.* 29, 1808994. doi:10.1002/adfm.201808994
- Ong, W.-J., Tan, L.-L., Ng, Y. H., Yong, S.-T., and Chai, S.-P. (2016). Graphitic carbon nitride (g-C₃N₄)-based photocatalysts for artificial photosynthesis and environmental remediation: are we a step closer to achieving sustainability? *Chem. Rev.* 116, 7159–7329. doi:10.1021/acs.chemrev.6b00075
- Rong, X., Liu, S., Xie, M., Liu, Z., Wu, Z., Zhou, X., et al. (2020). N₂ photofixation by Z-scheme single-layer g-C₃N₄/ZnFe₂O₄ for cleaner ammonia production. *Mater. Res. Bull.* 127, 110853. doi:10.1016/j.materresbull.2020.110853
- Shi, W., Li, M., Huang, X., Ren, H., Yan, C., and Guo, F. (2020a). Facile synthesis of 2D/2D Co₃(PO₄)₂/g-C₃N₄ heterojunction for highly photocatalytic overall water splitting under visible light. *Chem. Eng. J.* 382, 122960. doi:10.1016/j.cej.2019.122960
- Shi, W., Liu, C., Li, M., Lin, X., Guo, F., and Shi, J. (2020b). Fabrication of ternary Ag₃PO₄/Co₃(PO₄)₂/g-C₃N₄ heterostructure with following Type II and Z-scheme dual pathways for enhanced visible-light photocatalytic activity. *J. Hazard. Mater.* 389, 121907. doi:10.1016/j.jhazmat.2019.121907
- Shu, K., Chen, F., Shi, W., Guo, F., Tang, Y., Ren, H., et al. (2020). Construction of DyVO₄/nitrogen deficient g-C₃N₄ composite for enhanced visible-light photocatalytic activity for tetracycline degradation. *Mater. Res. Bull.* 124, 110766. doi:10.1016/j.materresbull.2020.110766

- Tahir, M., Cao, C., Mahmood, N., Butt, F. K., Mahmood, A., Idrees, F., et al. (2014). Multifunctional g-C₃N₄ Nanofibers: a template-free fabrication and enhanced optical, electrochemical, and photocatalyst properties. *ACS Appl. Mater. Interfaces* 6, 1258–1265. doi:10.1021/am405076b
- Wang, X., Maeda, K., Thomas, A., Takanahe, K., Xin, G., Carlsson, J. M., et al. (2009). A metal-free polymeric photocatalyst for hydrogen production from water under visible light. *Nature Mater.* 8, 76–80. doi:10.1038/nmat2317
- Wang, Y., Yao, J., Li, H., Su, D., and Antonietti, M. (2011). Highly selective hydrogenation of phenol and derivatives over a Pd@carbon nitride catalyst in aqueous media. *J. Am. Chem. Soc.* 133, 2362–2365. doi:10.1021/ja109856y
- Wang, Y., Wang, X., and Antonietti, M. (2012). Polymeric graphitic carbon nitride as a heterogeneous organocatalyst: from photochemistry to multipurpose catalysis to sustainable chemistry. *Angew. Chem. Int. Ed. Engl.* 51, 68–89. doi:10.1002/anie.201101182
- Wang, L., Zhu, C., Yin, L., and Huang, W. (2020). Construction of Pt-M (M = Co, Ni, Fe)/g-C₃N₄ composites for highly efficient photocatalytic H₂ generation. *Acta Phys. Chim. Sin.* 36, 1907001. doi:10.3866/pku.whxb201907001
- Wang, Y., Liu, J., Wang, Y., and Zhang, M. (2020a). CO₂ photoreduction to CO/CH₄ over Bi₂WO₆Mo_{0.5}O₆ solid solution nanotubes under visible light. *RSC Adv.* 10, 8821–8824. doi:10.1039/d0ra00672f
- Wang, Y., Shen, S. H., and Shen, S. (2020b). Progress and prospects of non-metal doped graphitic carbon nitride for improved photocatalytic performances. *Acta Phys. Chim. Sin.* 36, 1905080. doi:10.3866/pku.whxb201905080
- Wu, J. Q., Hua, W. M., Yue, Y. H., and Gao, Z. (2020). Swelling characteristics of g-C₃N₄ as base catalyst in liquid-phase reaction. *Acta Phys. Chim. Sin.* 36, 1904066. doi:10.3866/pku.whxb201912023
- Yan, S. C., Li, Z. S., and Zou, Z. G. (2010). Photodegradation of rhodamine B and methyl orange over boron-doped g-C₃N₄ under visible light irradiation. *Langmuir* 26, 3894–3901. doi:10.1021/la904023j
- Yang, Y., Chen, J., Mao, Z., An, N., Wang, D., and Fahlman, B. D. (2017). Ultrathin g-C₃N₄ nanosheets with an extended visible-light-responsive range for significant enhancement of photocatalysis. *RSC Adv.* 7, 2333–2341. doi:10.1039/c6ra26172h
- Yu, Z., Li, F., Yang, Q., Shi, H., Chen, Q., and Xu, M. (2017). Nature-mimic method to fabricate polydopamine/graphitic carbon nitride for enhancing photocatalytic degradation performance. *ACS Sustainable Chem. Eng.* 5, 7840–7850. doi:10.1021/acssuschemeng.7b01313
- Yu, C., He, H., Liu, X., Zeng, J., and Liu, Z. (2019). Novel SiO₂ nanoparticle-decorated BiOCl nanosheets exhibiting high photocatalytic performances for the removal of organic pollutants. *Chinese J. Catal.* 40, 1212–1221. doi:10.1016/s1872-2067(19)63359-0
- Zhang, D., Tan, G., Wang, M., Li, B., Dang, M., Ren, H., et al. (2020). The modulation of g-C₃N₄ energy band structure by excitons capture and dissociation. *Mater. Res. Bull.* 122, 110685. doi:10.1016/j.materresbull.2019.110685
- Zhang, P., Li, Y., Zhang, Y., Hou, R., Zhang, X., Xue, C., et al. (2020a). Photogenerated electron transfer process in heterojunctions: in situ irradiation XPS. *Small Methods* 4, 2000214. doi:10.1002/smt.202000214
- Zhang, P., Tong, Y., Liu, Y., Vequizo, J. J. M., Sun, H., Yang, C., et al. (2020b). Heteroatom dopants promote two-electron O₂ reduction for photocatalytic production of H₂ O₂ on polymeric carbon nitride. *Angew. Chem. Int. Ed. Engl.* 59, 16209–16217. doi:10.1002/anie.202006747
- Zhang, P., Zhang, S., Wan, D., Zhang, P., Zhang, Z., and Shao, G. (2020c). Multilevel polarization-fields enhanced capture and photocatalytic conversion of particulate matter over flexible schottky-junction nanofiber membranes. *J. Hazard. Mater.* 395, 122639. doi:10.1016/j.jhazmat.2020.122639
- Zhang, S., Zhang, P., Hou, R., Li, B., Zhang, Y., Liu, K., et al. (2020). In situ sulfur-doped graphene nanofiber network as efficient metal-free electrocatalyst for polysulfides redox reactions in lithium-sulfur batteries. *J. Energy Chem.* 47, 281–290. doi:10.1016/j.jechem.2020.01.033
- Zhang, Y., Zhang, P., Li, B., Zhang, S., Liu, K., Hou, R., et al. (2020). Vertically aligned graphene nanosheets on multi-yolk/shell structured TiC@C nanofibers for stable Li-S batteries. *Energy Storage Mater.* 27, 159–168. doi:10.1016/j.ensm.2020.01.029
- Zhao, S., Zhang, Y., Zhou, Y., Wang, Y., Qiu, K., Zhang, C., et al. (2018). Facile one-step synthesis of hollow mesoporous g-C₃N₄ spheres with ultrathin nanosheets for photoredox water splitting. *Carbon* 126, 247–256. doi:10.1016/j.carbon.2017.10.033
- Zheng, D., Pang, C., Liu, Y., and Wang, X. (2015). Shell-engineering of hollow g-C₃N₄ nanospheres via copolymerization for photocatalytic hydrogen evolution. *Chem. Commun.* 51, 9706–9709. doi:10.1039/c5cc03143e

Conflict of Interest: The authors declare that the research was conducted in the absence of any commercial or financial relationships that could be construed as a potential conflict of interest.

Copyright © 2021 Zhang, Sun, Chang and Zhang. This is an open-access article distributed under the terms of the Creative Commons Attribution License (CC BY). The use, distribution or reproduction in other forums is permitted, provided the original author(s) and the copyright owner(s) are credited and that the original publication in this journal is cited, in accordance with accepted academic practice. No use, distribution or reproduction is permitted which does not comply with these terms.